PERGAMON

International Journal of Heat and Mass Transfer 42 (1999) 1273–1287

International Journal of HEAT and MASS TRANSFER

Thermal conductance of cylindrical joints

Chakravarti V. Madhusudana

School of Mechanical and Manufacturing Engineering, The University of New South Wales, Sydney 2052, Australia

Received 24 February 1998; in final form 15 July 1998

Abstract

The heat flow across a joint formed by two concentric cylinders depends not only on the geometrical, thermophysical and surface properties of the cylinders but on the heat flux and maximum operating temperatures. An analysis is presented in which it is shown that, depending on the heat flow direction, the contact may be reinforced or completely relaxed during operation. These results are consistent with previous experimental observations of other workers in this area and recommendations of heat exchanger manufacturers. It is further shown that, because of the interdependence of the heat flux and the contact pressure, the exact nature of the correlation used for the solid spot thermal conductance becomes relatively unimportant.

Nomenclature

a inner radius of inner cylinder [m]
b radius of interface [m]
c outer radius of outer cylinder [m]
E modulus of elasticity [MPa]
h thermal contact conductance [W m^{-2} K^{-1}]
H microhardness of the softer material [MPa]
k harmonic mean of the solid thermal conductivities [W m^{-1} K^{-1}]
L length of cylinders [m]
p contact pressure [MPa]
q heat flux [W m^{-2}]
Q heat flow rate [W]
R thermal contact resistance [m^2 K^1 W^{-1}]
$\tan\theta$ mean absolute slope of surface profile, $\sqrt{(\tan^2\theta_i+\tan^2\theta_o)}$
T temperature [K]
u total interference between the cylinders [m]
u_A differential expansion due to temperature gradients [m]
u_B differential expansion due to contact resistance [m]
u_C initial interference [m].

Greek symbols

α coefficient of thermal expansion [K^{-1}]
δ_{eff} effective gap thickness [m]
ΔT temperature drop at the interface [K]
ν Poisson's ratio
σ effective rms surface roughness, $\sqrt{(\sigma_i^2+\sigma_o^2)}$ [m].

Subscripts

i inner cylinder
o outer cylinder
g gas
s solid.

1. Introduction

In many applications, the heat flow is radial across concentric compound cylinders. Examples include plug and ring assemblies, shrink-fit cylinders, finned tube heat exchangers, duplex and multiplex tubes used in solar thermal and nuclear power plants. Recent reviews of literature on heat flow through cylindrical joints have been presented by Madhusudana [1] and Ayers et al. [2]. These reviews point out the fact that, although cylindrical joints are just as commonplace as flat joints, the available literature on heat flow through cylindrical joints is comparatively small. A main reason for this appears to be the additional complexities that are present in such a situation.

In heat transfer across flat joints, the contact pressure is usually known (or estimated) and can be directly controlled. Hence, for a given joint, it is used as the independent variable and the thermal contact conductance is then expressed as the dependent variable. In a cylindrical joint, however, the contact pressure and, therefore, the contact conductance depend on the interference between

0017–9310/98/$ - see front matter
PII: S0017–9310(98)00239–7

the cylinders existing at the time of operation, see Williams and Madhusudana [3]. This interference consists of the following components:

(1) The differential expansion, u_A, due to the temperature gradients caused by the heat flow; u_A can be calculated using equations of thermoelasticity.
(2) The differential expansion, u_B, caused by the fact that, because of the contact resistance, the two surfaces at the interface will be at different temperatures.
(3) The interference, u_C, at the time of assembly (that is, the initial degree of fit).

It can be seen that u_A depends on the heat flux and u_B depends on both the heat flux and the operating temperatures. The heat flux, or some measure of it, and the maximum temperatures are, therefore, the primary variables controlling the contact conductance of a given pair of cylinders.

In this paper, steps needed to estimate the joint conductance of compound cylinders will be described first. Results for typical configurations will then be presented to illustrate the effects of parameters such as heat flux, the maximum temperature, material combinations, and the surface characteristics. The significance of these results will then be discussed in light of previous observations and recommendations.

It may be noted that a few preliminary analyses of the thermal behaviour of cylindrical joints have been previously published. Novikov et al. [4], for example, considered the contact of coaxial cylinders in vacuum. Madhusudana [5], Lemczyk and Yovanovich [6] and Egorov et al. [7] analysed the effect of the heat flux on conductance of cylindrical joints. Other works are noted in the reviews [1, 2] listed above. One of the significant features of the present paper is including the effect of maximum temperature rise on thermal contact conductance. This aspect does not seem to have been considered by any of these previous works. Another objective of the present paper is to demonstrate the influence of the numerous design parameters and operating conditions that influence the contact pressure and contact conductance in a cylindrical joint.

1.1. Statement of the problem

Consider the compound cylinder shown in Fig. 1. The interface radius is b. Heat flow is taken to be radially outward. Because of the ever present microscopic and macroscopic surface irregularities, such as surface roughness and waviness, the contact between the two surfaces at the joint is necessarily imperfect. As a result, a finite resistance to heat flow exists at the interface. This thermal contact resistance, R, may be defined as:

$$R = \Delta T/q \tag{1}$$

in which ΔT is the temperature drop at the interface, and

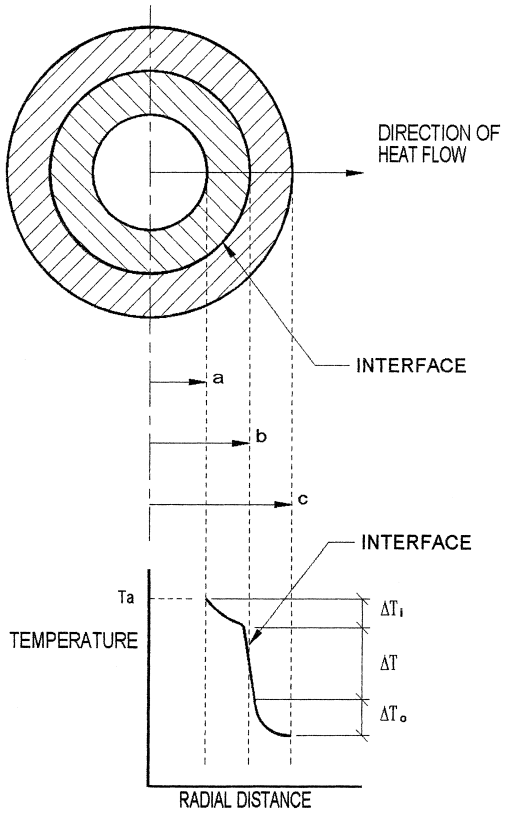

Fig. 1. Radial heat flow in a cylindrical joint.

q is the heat flux at the interface. The thermal contact conductance, h, is the reciprocal of R.

The heat flow through the joint occurs mainly through the solid spots in actual contact and through the medium, such as air, filling the interstices between the adjacent contact spots. The contact conductance, therefore, consists mainly of two components: the solid spot conductance and the gas gap conductance. At high temperatures, the contribution by radiation may become significant and the contact conductance need to be modified accordingly. The present analysis uses a widely accepted theoretical expression for the estimation of the solid spot conductance. However, the effect of using an empirical correlation based on experimental data is also explored.

2. Analysis

Referring to Fig. 1, the pressure developed between the two cylinders, as a result of the interference u between them, is given by [8]:

$$\frac{u}{b}=\frac{p}{E_i}\left\{\frac{E_i}{E_o}\left[\frac{c^2+b^2}{c^2-b^2}+\nu_o\right]+\left[\frac{b^2+a^2}{b^2-a^2}+\nu_i\right]\right\} \tag{2}$$

or

$$\frac{u}{b}=\frac{p}{E_i}\{C_1\} \tag{2a}$$

in which

$u = u_A + u_B + u_C$

and C_1 is the term inside the braces { } in equation (2).

For a given pair of cylinders, the initial interference, u_C, is known. The differential expansions, u_B and u_A, need to be determined from the conditions of heat flow.

The steady state heat flow is:

$$Q=\frac{2\pi Lk_i\Delta T_i}{\ln(b/a)}=\frac{2\pi Lk_o\Delta T_o}{\ln(c/b)} \tag{3}$$

in which L is the length of the composite cylinder.

From equation (3)

$$\Delta T_o=\left(\frac{k_i}{k_o}\right)\left[\frac{\ln(c/b)}{\ln(b/a)}\right]\Delta T_i. \tag{4}$$

2.1. Interference due to the flow of heat

The heat flow results in the deformations of the cylinders. At the interface, the radial displacements of the inner and outer cylinders are, respectively, [9]:

$$u_{Ai}=\frac{b\alpha\Delta T_i}{2\ln(b/a)}\left[1-\frac{2a^2}{b^2-a^2}\ln(b/a)\right] \tag{5a}$$

$$u_{Ao}=\frac{b\alpha_o\Delta T_o}{2\ln(c/b)}\left[1-\frac{2c^2}{c^2-b^2}\ln(c/b)\right]. \tag{5b}$$

Substituting for ΔT_o from equation (4),

$$u_{Ao}=\frac{b\alpha_o}{2\ln(c/b)}\left[1-\frac{2c^2}{c^2-b^2}\ln(c/b)\right]\left(\frac{k_i}{k_o}\right)\left[\frac{\ln(c/b)}{\ln(b/a)}\right]\Delta T_i$$

$$=\frac{b\alpha_i\Delta T_i}{2\ln(b/a)}\left(\frac{\alpha_o k_i}{\alpha_i k_o}\right)\left[1-\frac{2c^2}{c^2-b^2}\ln(c/b)\right]. \tag{5c}$$

Since the net interference due to heat flow is

$u_A = u_{Ai} - u_{Ao}$

we can write

$$(u_A/b)=\Delta T_i(C_2) \tag{6}$$

where

$$C_2=\frac{\alpha_i}{2\ln(b/a)}\left\{\left[1-\frac{2a^2}{b^2-a^2}\ln(b/a)\right]-\left(\frac{\alpha_o k_i}{\alpha_i k_o}\right)\left[1-\frac{2c^2}{c^2-b^2}\ln(c/b)\right]\right\}. \tag{6a}$$

2.2. Interference due to contact resistance

Because of the finite resistance to the heat flow at the joint, the two sides of the interface will be at different temperatures. The consequent differential expansion is:

$$u_B = u_{Bi} - u_{Bo}$$
$$= b\alpha_i T_1 - b\alpha_o(T_1-\Delta T)$$
$$= b[T_1(\alpha_i-\alpha_o)+\alpha_o\Delta T)]$$

where T_1 is the temperature rise of the outer surface of the inner cylinder.

Thus,

$$u_B=b[(T_a-\Delta T_i)(\alpha_i-\alpha_o)+\alpha_o\Delta T)] \tag{7}$$

Note:

(1) T_a refers to the temperature of the inner surface of the inner cylinder, that is, to the maximum temperature of the assembly. This is measured with respect to the temperature, T_∞, at which the dimensions of the cylinders were established (e.g., the room temperature) as the datum. In other words, $T_a = T_{max} - T_\infty$, is the *maximum temperature rise* over the initial temperature.

(2) If both the cylinders are made of the same material (or, at least, have the same coefficient of thermal expansion) the first term inside the brackets of equation (7) reduces to zero. Thus, in this case, the maximum temperature has no significance.

In equation (7),

$\Delta T = q/h$

and

q = heat flux at the interface

$$= Q/A=\frac{2\pi k_i L\Delta T_i}{\ln(b/a)}\frac{1}{2\pi bL}$$

where $2\pi bL$ is the heat flow area, A, at the interface.

Thus,

$$q=\frac{k_i\Delta T_i}{b\ln(b/a)} \tag{7a}$$

and

$h = h_s + h_g$

in which h_s and h_g are the solid spot and the gas gap conductances, respectively.

The solid spot conductance for ideal, flat, rough surfaces is given by [10]:

$$h_s=1.13\tan\theta(k/\sigma)(p/H)^{0.94}. \tag{7b}$$

For practical surfaces, which contain some degree of flatness deviation and/or waviness, empirical correlations exist for the estimation of the solid spot conductance. One such correlation is [11]:

$$h_s=0.55\tan\theta(k/\sigma)(p/H)^{0.85}. \tag{7c}$$

Thus, in general, we can write:

$$h_s=C_3\tan\theta(k/\sigma)(p/H)^n. \tag{7d}$$

The gas gap conductance, h_g, can be calculated as:

$$h_g=k_g/\delta_{eff}. \tag{7e}$$

The effective thickness of the gas gap, δ_{eff}, must take into

account both the dimensions of the physical gap as well as the 'temperature jump distance' [12]. Previous works indicate that the effective thickness is approximately equal to 3σ, see for example [13, 14]. However, no numerical values need to be assumed during the derivation.

Equation (7) can, therefore, be written as:

$$u_B/b = C_4(T_a - \Delta T_i) + \alpha_o \frac{k_i \Delta T_i}{b \ln(b/a)} \left[\frac{1}{C_3 \tan\theta (k/\sigma)(p/H)^n + (k_g/\delta_{eff})} \right]$$

$$u_B/b = C_4(T_a - \Delta T_i) + C_5 \left[\frac{1}{C_6 p^n + C_7} \right] \Delta T_i \quad (8)$$

where

$$C_4 = (\alpha_i - \alpha_o)$$

$$C_5 = \frac{k_i}{b \ln(b/a)}$$

$$C_6 = C_3 \tan\theta (k/\sigma)(1/H)^n$$

$$C_7 = k_g/\delta_{eff}.$$

Substituting for u_A and u_B in equation (2), we notice that, for a given pair of cylinders:

(1) The differential expansion depends on both the heat flux (as given by ΔT_i), and the maximum temperature rise;

(2) The contact pressure p appears on both sides of the equation. Hence an iterative method would be required to solve for the pressure and, hence, the thermal contact conductance.

Table 1
Material properties used in the presentation of theoretical results

Material	Stainless steel	Material
Thermal conductivity ($W\,m^{-1}\,K^{-1}$)	16.5	200
Coefficient of expansion, α ($10^{-6}\,K^{-1}$)	18	24
Modulus of elasticity, E (GPa)	200	70
Poisson's ratio	0.28	0.33
Microhardness (MPa)	2750	1400

3. Discussion

In a flat joint, the relationship between the conductances and the factors affecting them is direct and it is easy to visualise the effect of each variable on the contact conductance, see equations (7). In a cylindrical joint, as is evident from the above analysis, the contact pressure itself is controlled by the material and geometric parameters as well as the heat flux and the maximum temperature. Because of this implicit relationship between the conductance and the system parameters, it is convenient to plot the results graphically for typical ranges of variables in order to understand their influence. In generating the following set of graphs, the radii a, b and c are taken to be 9, 10 and 11 mm, respectively and the material properties are summarised in Table 1. In all cases, heat flow direction is taken to be radially outward. The interface medium is taken to be air.

The results are summarised in Figs 2–9. The relevant parameters used in generating the graphs of Figs 2–8 are listed in Table 2.

3.1. Stainless steel → aluminium joint

Figure 2(a) illustrates the variation of contact pressure with the maximum temperature rise, for the above joint assembled with a nominal zero interference. Because of the differential expansion of the two cylinders, and since α_{ss} is less than α_{al}, it is seen that the contact pressure gradually decreases as the maximum temperature decreases. The exact temperature at which the contact pressure becomes zero, for a given pair of cylinders, depends on the heat flux as measured by ΔT_i, the temperature drop across the wall of the inner cylinder; the

Table 2
Parameters used in generating Figs 2–8

Figure number	Material combination	Interference (u_c/b)	Surface roughness (μm)	Surface slope (°)	Heat flux (ΔT_i) (K)
2	ss → al	0	3	10	Various
3	al → ss	0	3	10	Various
4	ss → ss	0 and 0.0005	3	10	Variable
	al → al	0 and 0.0005	3	10	Variable
5	Various	0	1	5	Variable
6	ss → al	0.0005	Variable	10	5
7	ss → al	0.0005	3	Variable	5
8	ss → al	0	1	10	10

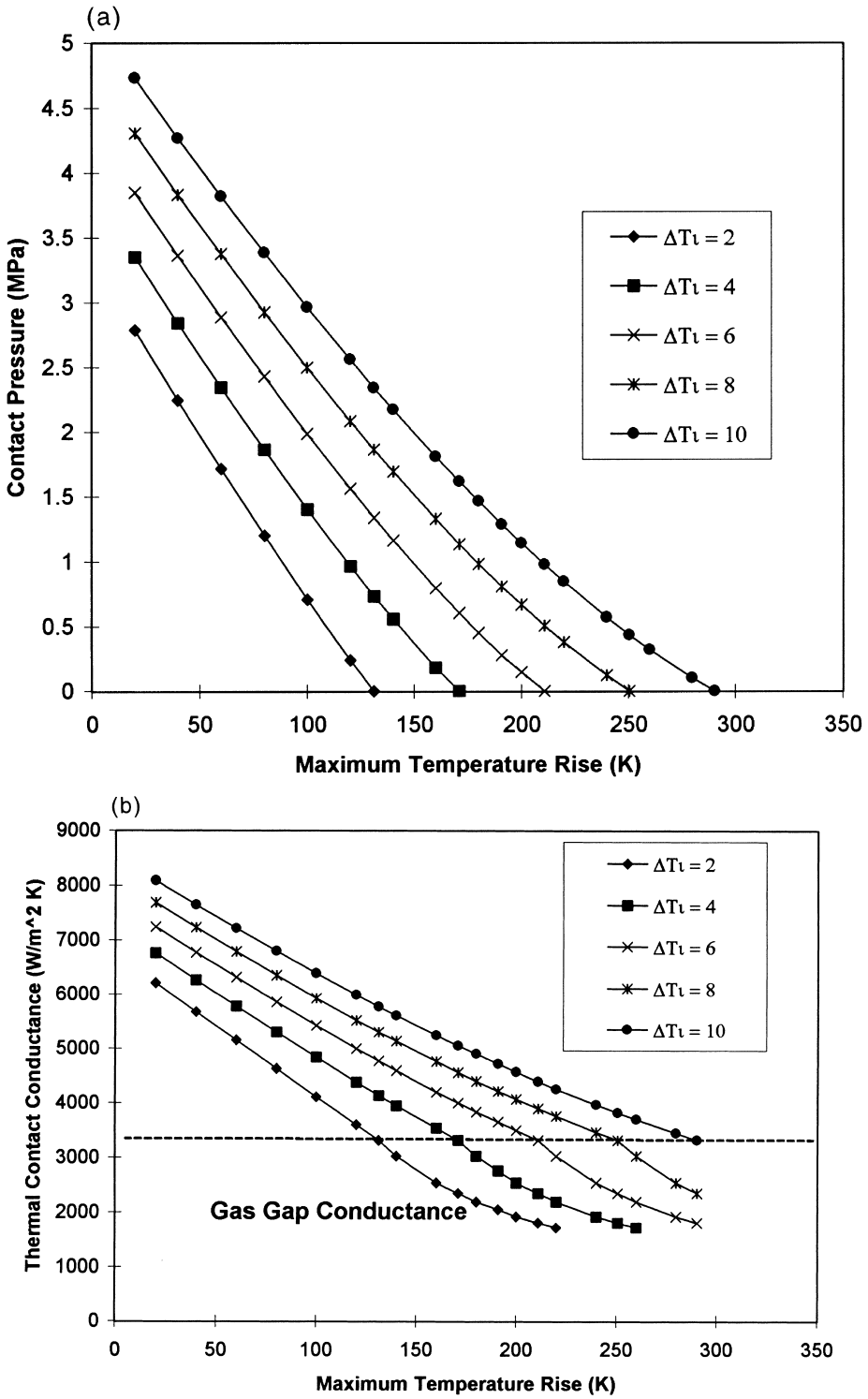

Fig. 2. Stainless steel–aluminium joint [$\sigma = 3$ μm; $\theta = 10°$; $(u_c/b) = 0$]: (a) variation of contact pressure with maximum temperature rise; (b) variation of contact conductance with maximum temperature rise.

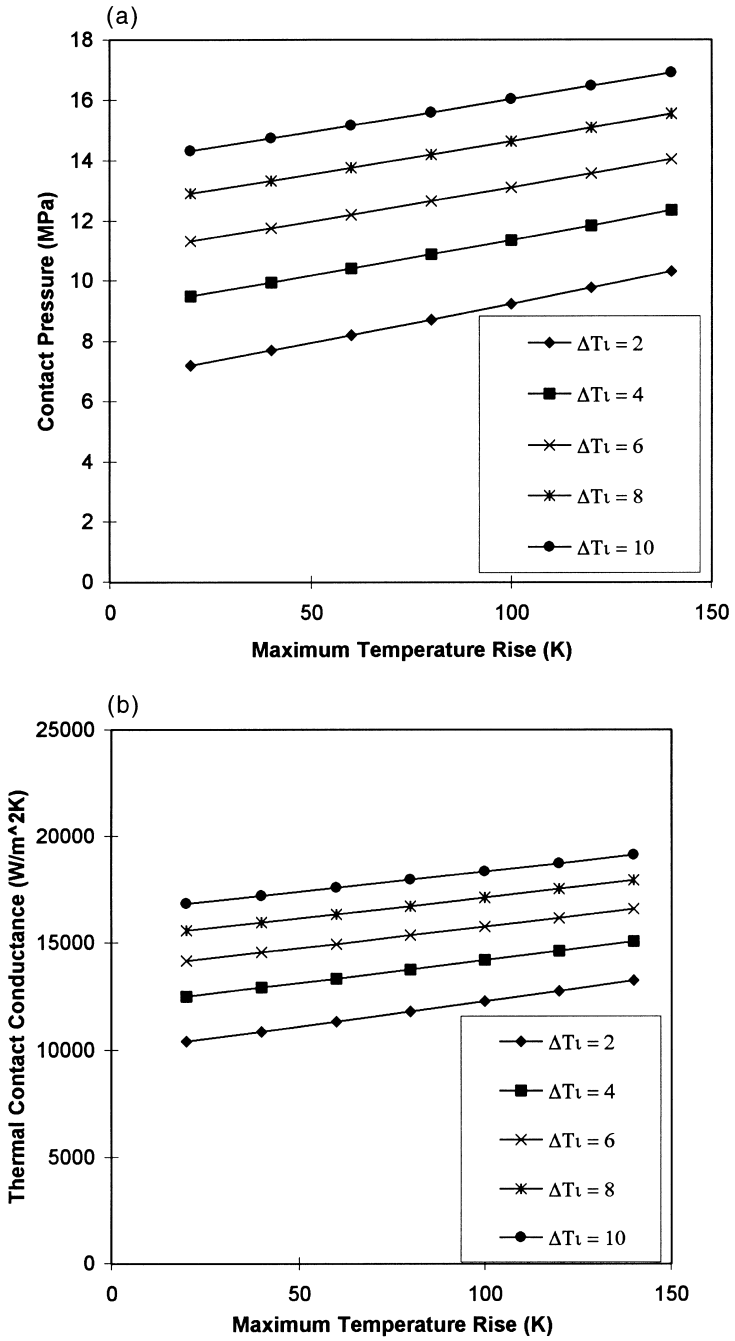

Fig. 3. Aluminium–stainless steel joint [$\sigma = 3$ μm; $\theta = 10^{\circ}$; $(u_c/b) = 0$]: (a) variation of contact pressure with maximum temperature rise; (b) variation of contact conductance with maximum temperature rise.

greater the heat flux, the greater is the temperature at which the pressure is completely relaxed. The contact conductance is also correspondingly decreased and, when the contact pressure is zero, it attains the value of the air gap conductance for zero clearance. This is indicated by the dashed line in Fig. 2(b). Further increase in temperature will increase the gap and further decrease the gap conductance.

These results are in agreement with the observations of Gardner and Carnavos [15] who noted that, for alu-

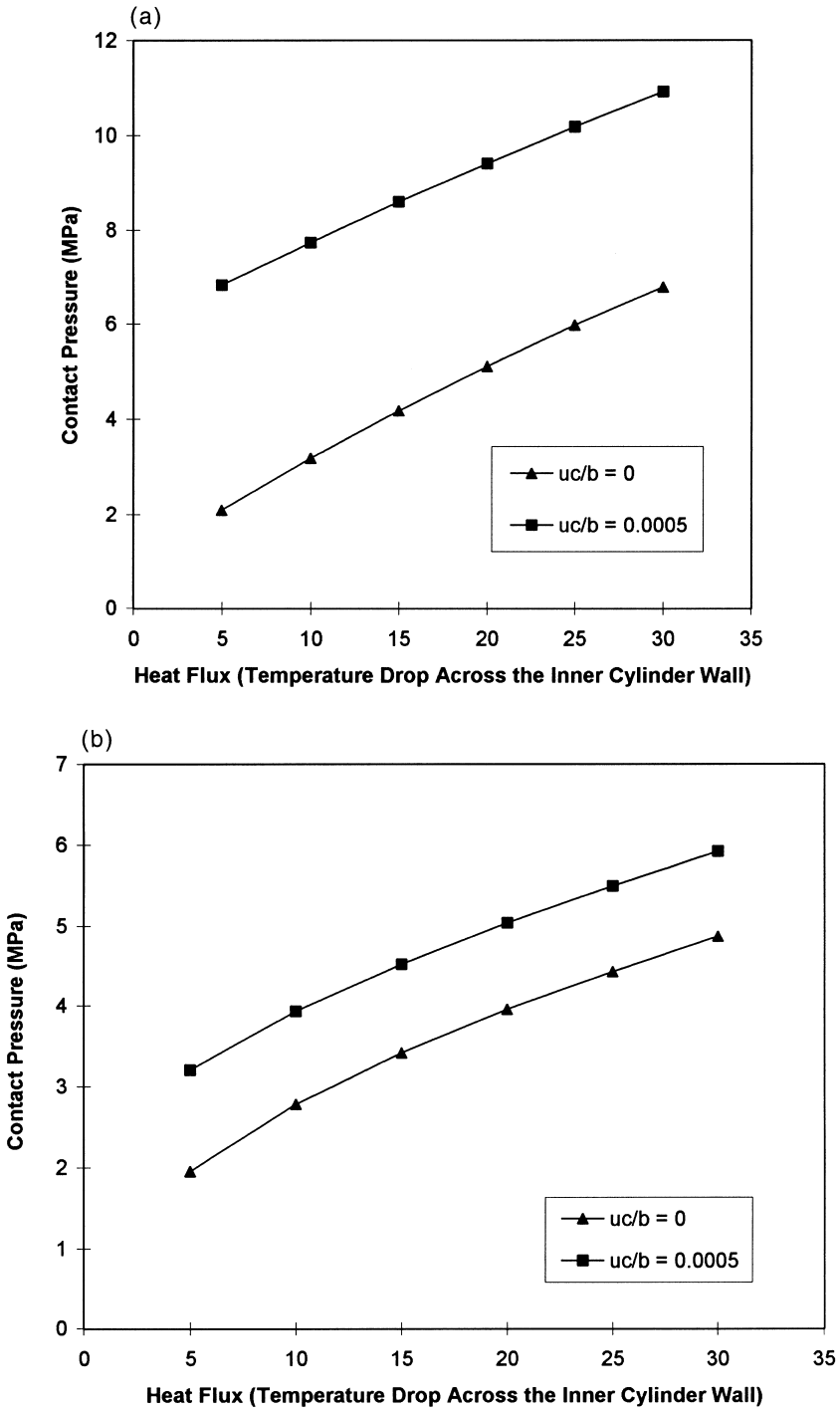

Fig. 4. Similar materials; variation of contact pressure with heat flux [$\sigma = 3$ μm; $\theta = 10°$]: (a) stainless steel–stainless steel; (b) aluminium–aluminium.

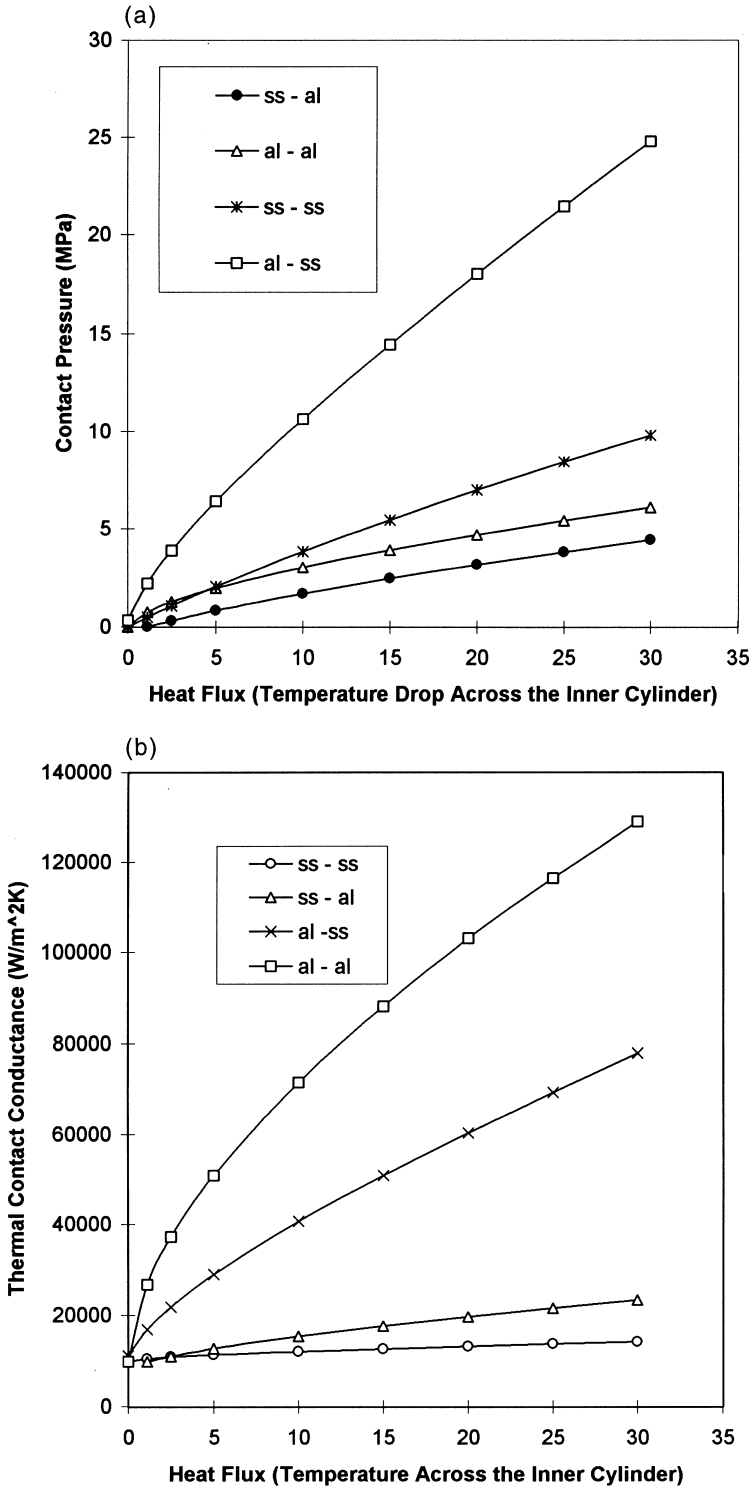

Fig. 5. Effect of the material combination [$\sigma = 1$ μm; $\theta = 5^{\circ}$; $(u_c/b = 0]$: (a) contact pressure variation with heat flux; (b) contact conductance variation with heat flux.

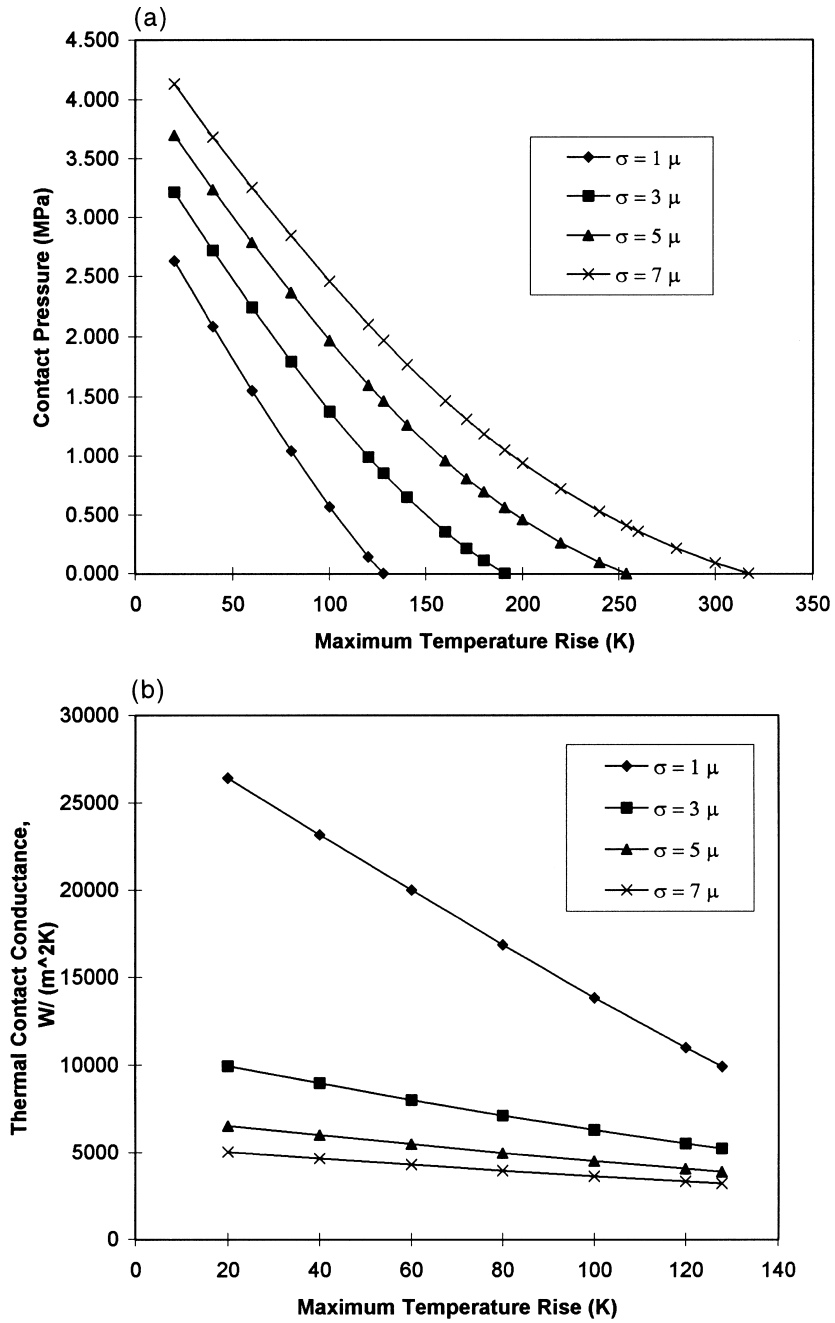

Fig. 6. Effect of varying the surface roughness [$\Delta T_i = 5$ K; $\theta = 10^\circ$; $(u_c/b) = 0.0005$]: (a) contact pressure variation with maximum temperature rise; (b) contact conductance variation with maximum temperature rise.

minium finned steel tubes, at high temperatures (typically 125 to 140 C) the contact pressure between the fin and the tube will be relaxed to such an extent that the gap resistance becomes significant. In his discussion of shoulder ('L-foot'), and extruded finned tubes, Taborek [16] also noted that, if the thermal coefficient of expansion of the fin material is larger than that of the base, then the contact between the two materials will loosen as the temperature increases and the bond resistance will increase. He also noted that this was, unfortunately, true for the

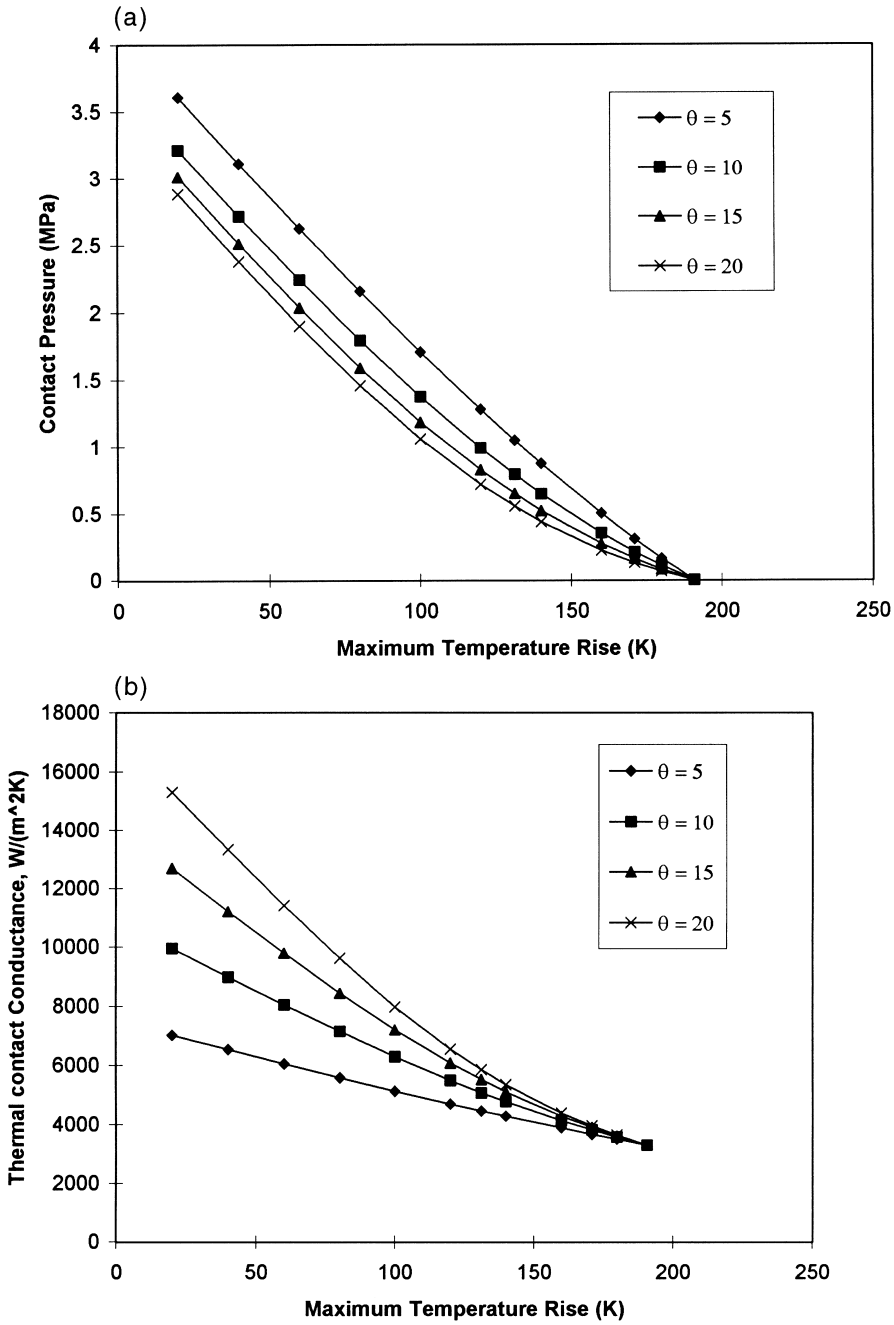

Fig. 7. Effect of varying the surface slope [$\Delta T_i = 5$ K; $\sigma = 3$ μm; $(u_c/b) = 0.0005$]: (a) contact pressure variation with maximum temperature rise; (b) contact conductance variation with maximum temperature rise.

usual combination of aluminium fin and virtually any other tube material, especially for the common case of carbon steel. This is one of the reasons for specifying the current maximum operating temperatures for finned tubing (Data from [16]) as indicated in Table 3.

3.2. *Aluminium → stainless steel*

By contrast, the contact pressure is reinforced with increase in temperature when the inner tube material has a higher coefficient of expansion, as seen in Fig. 3(a). The

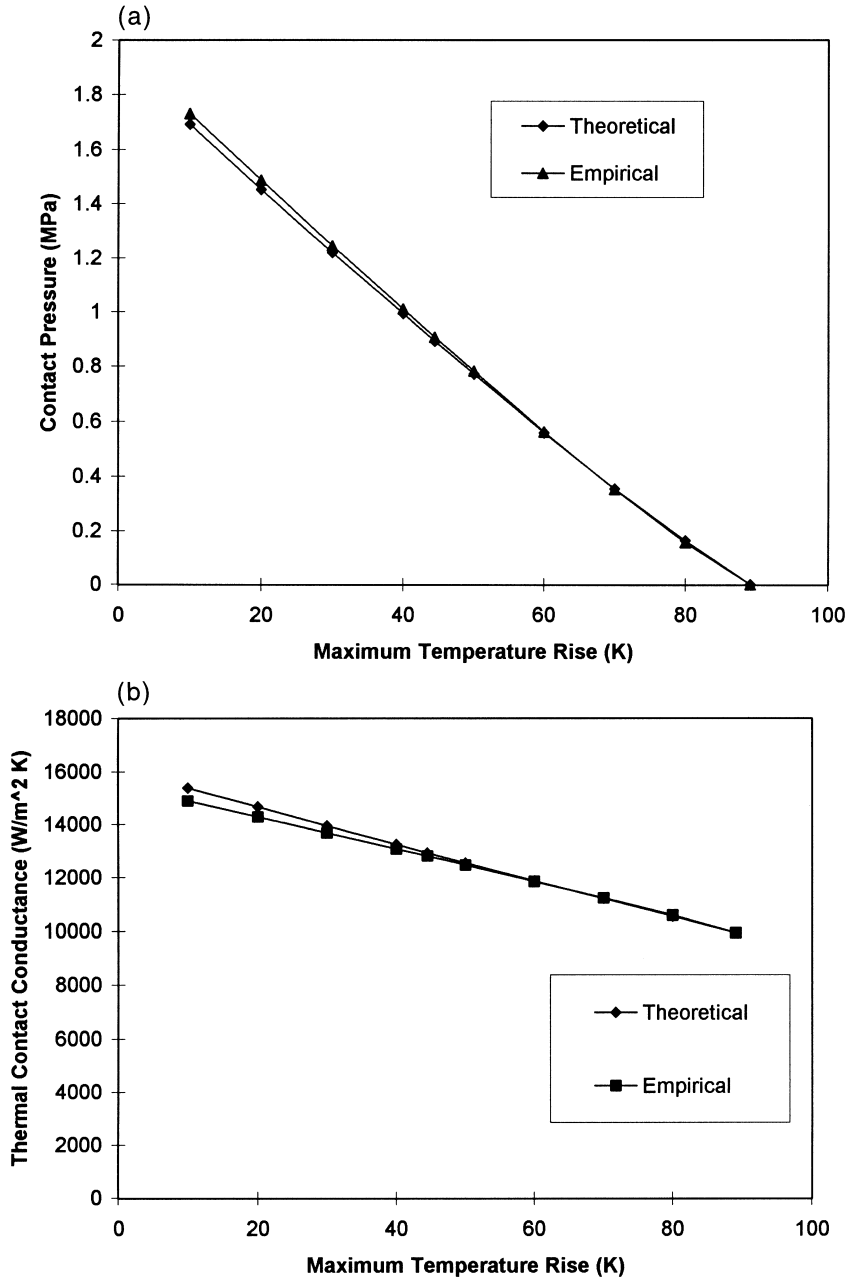

Fig. 8. Results of varying the correlation for the solid spot conductance [$\sigma = 1$ μm; $\theta = 10^{\circ}$; $(u_c/b) = 0$; $\Delta T_i = 10$ K]: (a) contact pressure variation with maximum temperature rise; (b) contact conductance variation with maximum temperature rise.

contact conductance also increases correspondingly, see Fig. 3(b). The amount of such increases is again very much influenced by the heat flux, which is the other parameter in Figs 3(a) and (b). These observations, it should be remembered, apply to radially outward heat flow. Condenser tubes, failed due to erosion or corrosion, may be returned to service by means of lining, that is, insertion of very thin metallic tubing which is expanded in situ by the application of hydraulic pressure [17]. In such a lined condenser tubing, the heat flow is radially inward. In such a case, the use of a liner made of 90–10 copper–nickel alloy ($\alpha = 17 \times 10^{-6}$) or 70–30 copper–nickel alloy ($\alpha = 16 \times 10^{-6}$) inside an aluminium brass tubing ($\alpha = 19 \times 10^{-6}$) will result in the reinforcement of contact during operation [18].

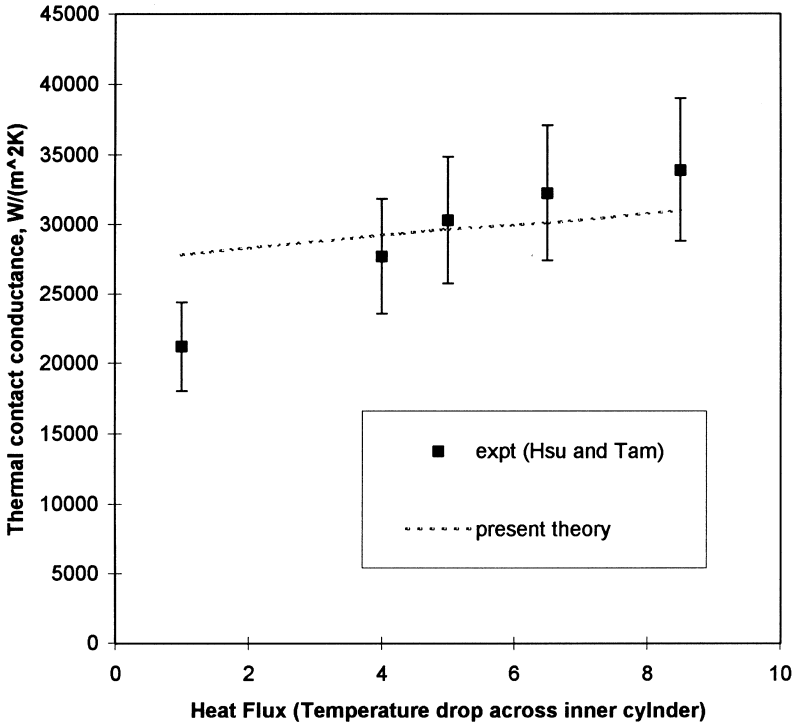

Fig. 9. Comparison of present theory with previous experimental results.

Table 3
Recommended maximum operating temperatures for finned tubing

Type of finned tubing	U.S. practice	European practice
L-footed tubes	176 C	150 C
Extruded tubes	230 C	250 C

3.2.1. Similar materials

As indicated, in the analysis, the maximum temperature does not contribute to the differential expansion in the case of materials with the same coefficient of expansion. The results for stainless steel → stainless steel and aluminium → aluminium, in Figs 4(a) and (b), respectively, are therefore plotted with the heat flux as the independent variable. It can be seen that:

- the contact pressure increases as the heat flux increases.
- a slight interference will cause a noticeable increase in the contact pressure.

It may be readily seen that the contact conductance would exhibit similar trends.

3.3. Material combination

The contact pressure and the contact conductance developed for the four different material combination are depicted in Figs 5(a) and (b). The independent variable is again taken as the heat flux. For the dissimilar material combinations, the maximum temperature rise is taken to be 10 K (the temperature rise is irrelevant for similar materials). In all cases, the initial interference is taken to be zero.

It is apparent that the material combination enormously influences the contact pressure and contact conductance. As expected, the largest contact pressures are developed for the aluminium → stainless steel combination and the smallest pressures for stainless steel → aluminium combination. The pressures developed for aluminium → aluminium joint are the second lowest; however, this joint still develops the maximum conductance because of the high effective conductivity of the joint forming materials. It is particularly interesting to observe the results for stainless steel → aluminium and aluminium → stainless steel combinations. Although

these have the same effective conductivity, yet the conductance of the latter is almost twice that of the former! This indicates the importance of the direction of heat flow, whether it is from a material of lower α to one of higher α or vice versa. In other words, some kind of 'rectification' can be seen to exist for heat flow in cylindrical joints formed by different materials.

In Fig. 5(a), the contact pressure for similar materials becomes zero at zero heat flux. For dissimilar materials, the contact pressure also depends on the temperature rise. For the temperature rise (10 K) applicable to this figure, the contact pressure for the stainless steel → aluminium joint becomes zero for $\Delta T_1 = 1.12$ K; for the aluminium → stainless steel joint, there still exists a small contact pressure of 0.345 MPa when the heat flux is zero. As indicated in Fig. 5(b), the conductance values for all combinations become equal to the gas gap conductance when the contact pressure becomes zero.

3.4. Surface characteristics

The effect of varying the surface roughness, for a given joint, on the contact pressure and the contact conductance are shown in figs 6(a) and (b). It is seen that, at any temperature, an increase in roughness will result in an increase in contact pressure, but a decrease in conductance. Conversely, an increase in surface slope will cause lower contact pressures and higher contact conductances, as indicated in Figs 7(a) and (b). These latter figures indicate that the surface slope is an important parameter that needs to be identified in contact conductance investigations. Most early works do not contain information on the slope. It may, however, be noted that, in general, the surface roughness and surface slope are not completely independent of each other.

3.5. Effect of correlation used

Figures 8(a) and (b), respectively compare the contact pressure and the contact conductance developed for the stainless steel → aluminium joint using the two expressions, given in equations 7(b) and (c), for the solid spot conductance. It can be seen that the empirical correlation gives a slightly higher contact pressure and a slightly lower contact conductance compared to the results obtained using the theoretical correlation. In fact, the difference is negligibly small for most practical purposes. The reason, of course, is that the contact conductance and contact pressure are strongly interdependent in the case of cylindrical joints. For flat joints, the two results would be noticeably different.

3.6. Comparison with previous experimental work

There are very few experimental works which deal with systematic, general study of heat flow in cylindrical joints. One such study is that of Hsu and Tam [19]. Figure 9 compares their results with those obtained using the present analysis. Table 4 summarises the data applicable to these tests.

No information was given regarding the mean slope of the surface profile. However, it was stated that the outside surface of the aluminium cylinder was turned to the desired roughness. In the eight measurements reported by Chetwynd [20], the slope for fine turned surfaces varied between 0.054–0.141. In the present calculations, an average value 0.105 (corresponding to $\theta = 6^\circ$) has, therefore, been assumed for the effective slope. It may also be noted that, in these tests, a change in heat flux also resulted in a change in the maximum temperature rise as indicated below:

ΔT_i (K)	1	4	5	6.5	8.5
T_a (K)	3	14	17.5	21.5	28.5

It may be seen that the test results show good agreement with the theory. The error bands on the experimental data indicate the uncertainties ($\pm 15\%$) as presented by Hsu and Tam. The slopes of the experimental and theoretical graphs, however, are seen to differ. A possible explanation is the almost certain existence of out-of-roundness and waviness in the actual test surfaces. These errors of form introduce a macroscopic constriction resistance in addition to the microscopic constriction resistance due to the surface roughness [21]. As the temperature and heat flux are increased, both microscopic and macroscopic resistances decrease simultaneously. It, therefore, follows that the slope of the experimental conductance vs. heat flux graph is higher than that of the theoretical one. The contact conductance

Table 4
Material, surface and geometric data applicable to the tests of Hsu and Tam [19]

	Inner cylinder	Outer cylinder
Material	Alclad 2011-T351	Stainless steel, AISI 304
Modulus of elasticity (GPa)	71	200
Thermal conductivity ($W m^{-1} K^{-1}$)	155	16.5
Coefficient of expansion (K^{-1})	22.8 (10^{-6})	17.3 (10^{-6})
Microhardness (MPa)	933	2420
Poisson's ratio	0.28	0.33
Surface roughness (μm)	3–4.8	1.27–1.65
Inner radius (mm)	11	29.58
Outer radius (mm)	29.58 + 0.0254	36.26

results of Hsu and Tam have been presented against contact pressure in a previous work [6]. It is to be emphasised, however, that the contact pressure is not an independent variable. In fact, it is estimated from the theory which would be used to predict the contact conductance. The independently controlled (and directly measured) heat flux is, therefore, the proper parameter against which the contact conductance needs to be plotted and compared with theoretical predictions.

It would be, indeed, desirable to test the theory against further experimental data if they were available. The experimental results reported by earlier workers, however, do not contain significant data such as maximum temperature and slope and, in some cases, even surface roughness. Theoretical estimates in such instances would, therefore, be impossible unless a large number of assumptions are made.

4. Conclusions

An analysis has been presented for the prediction of the thermal conductance of cylindrical joints for radial heat flow. This theory takes into account the differential expansion of the concentric cylinders due to the temperature gradients caused by heat flow, the maximum operating temperature and the finite temperature drop due to the contact resistance at the interface. It is shown that material combinations, geometric dimensions of the cylinders, surface characteristics and the properties of the interstitial medium also affect the joint thermal conductance.

It is found that, in general, the contact conductance of a given joint is influenced by both the heat flux and the maximum operating temperature. For similar materials at moderate temperatures, however, the contact conductance is independent of the maximum temperature.

Depending on the material combination, the contact may either be reinforced or become completely relaxed during operation. The latter condition forms one of the bases for specifying the maximum operating temperature of finned tubing used in heat exchangers.

For the same material combination, that is, for the same effective thermal conductivity of the joint materials, the conductance obtained could be vastly different depending on the direction of the heat flow in a cylindrical joint.

The conductance of a cylindrical joint is largely insensitive to the type of correlation used for the solid spot conductance.

The theoretically estimated results show reasonable agreement with the experimental data of other investigators.

It is recommended that reports of future experiments on cylindrical joints include detailed description of surface parameters as well as the maximum temperature rise encountered in the tests.

References

[1] C.V. Madhusudana, Thermal Contact Conductance, 1st ed., Springer-Verlag, New York, 1996, pp. 115–117.
[2] G.H. Ayers, L.S. Fletcher, C.V. Madhusudana, A review of thermal contact conductance of composite cylinders, Journal of Thermophysics and Heat Transfer 11 (1997) 72–81.
[3] A. Williams, C.V. Madhusudana, Heat flow across cylindrical metallic joints, Proceedings of the 4th International Heat Transfer Conference, vol. 3, Elsevier, Amsterdam, 1970, p. Cu 3.6.
[4] I.I. Novikov, L.S. Kokorev, N.N. Del'vin, Experimental heat exchange between coaxial cylinders in vacuum, Atomnaya Energiya 32 (1972) 474–475.
[5] C.V. Madhusudana, On heat flow across cylindrical joints, Proceedings of the 8th International Heat Transfer Conference, vol. 2, Hemisphere, New York, 1986, p. 651–658.
[6] T.F. Lemczyk, M.M. Yovanovich, New models and methodology for predicting thermal contact resistance of compound tubes and finned tubes, Heat Transfer Engineering 8 (1987) 35–48.
[7] E.D. Egorov, M.I. Nekrasov, V.Yu Pikus, A.A. Daschchyan, Investigation of contact heat-transfer resistance in two layer finned tubes, Energomashinostroenie 6 (1989) 17–19.
[8] A.C. Ugural, S.K. Fenster, Advanced Strength and Applied Elasticity, Elsevier, New York, 1975, pp. 255–256.
[9] S.P. Timoshenko, J.N. Goodier, Theory of Elasticity, 3rd ed., McGraw-Hill, New York, 1970, pp. 443–450.
[10] B.B. Mikic, Thermal contact conductance: theoretical considerations, International Journal of Heat and Mass Transfer 17 (1974) 205–214.
[11] C.L. Tien, A correlation for thermal contact conductance of nominally flat surfaces in vacuum, Proceedings of the 7th Conference on Thermal conductivity, U.S. National Bureau of Standards, Gaithersburg, 1972, pp. 755–759.
[12] E.H. Kennard, Kinetic Theory of Gases, McGraw-Hill, New York, 1938, pp. 311–320.
[13] T. Tsukizoe, T. Hisakado, On the mechanism of contact between metal surfaces—the penetrating depth and the average clearance, Transactions of the ASME, Journal of Basic Engineering 87 (1965) 666–674.
[14] V.M. Popov, A.I. Krasnoborod'ko., Thermal contact resistance in a gaseous medium, Inzhenerno-Fizicheski Zhurnal 28 (1975) 875–883.
[15] K.A. Gardner, T.C. Carnavos, Thermal contact resistance in finned tubing, Transactions of the ASME, Journal of Heat Transfer 82 (1960) 279–293.
[16] J. Taborek, Bond resistance and design temperatures for high-finned tubes—a reappraisal, Heat Transfer Engineering 8 (1987) 26–34.
[17] C.P. Tallman (Sr), Extend heat exchanger and condenser life with metal alloy inserts, in: J.R. Maurer (Ed.), Performance Monitoring and Replacement of Heat Exchanger

Components and Materials, ASME, New York, 1990, pp. 45–50.
[18] M.E. Rich, C.V. Madhusudana, Heat transfer performance of lined condenser tubes, Paper presented at the 6th Australasian Heat and Mass Transfer Conference, Sydney, 1996, unpublished.
[19] T.R. Hsu, W.K. Tam, On thermal contact resistance of compound cylinders, Paper 79-1069, AIAA 14th Thermophysics Conference, Orlando, FL, 1979.
[20] D.G. Chetwynd, Slope measurement in surface texture analysis, J. Mechanical Engineering Science 20 (1978) 115–119.
[21] A.M. Clausing, B.T. Chao, Thermal contact resistance in a vacuum environment, Trans. ASME, J. Heat Transfer 87 (1965) 243–251.